archives
of thermodynamics
Vol. **35**(2014), No. 2, 21–36
DOI:10.2478/aoter-2014-0011

Comparison of selected theoretical models of bubble formation and experimental results

MARIUSZ R. RZĄSA[1]

Opole University of Technology, Mikołajczyka 5, 45-271 Opole, Poland

Abstract Designers of all types of equipment applied in oxygenation and aeration need to get to know the mechanism behind the gas bubble formation. This paper presents a measurement method used for determination of parameters of bubbles forming at jet attachment from which the bubles are displaced upward. The measuring system is based on an optical tomograph containing five projections. An image from the tomograph contains shapes of the forming bubbles and determine their volumes and formation rate. Additionally, this paper presents selected theoretical models known from literature. The measurement results have been compared with simple theoretical models predictions. The paper also contains a study of the potential to apply the presented method for determination of bubble structures and observation of intermediate states.

Keywords: Bubble formation; Optical tomography; Bubble flow measurement

Nomenclature

C_D	–	drag coefficient
d	–	bubble diameter
d_E	–	dimensionless diameter of the bubble
d_o	–	orifice diameter
F_B	–	buoyancy force
F_D	–	drag force
F_I	–	inertia force
F_p	–	liquid pressure force
F_σ	–	surface tension force

[1]E-mail: m.rzasa@po.opole.pl

Fr – Froude number
g – gravitational acceleration
Q – gas flow
Re – Reynolds number
t – time
We – Weber number
v – velocity of bubble mass center
x – distance between the bubble centre and the nozzle

Greek symbols

ρ_l – density of liquid
ρ_g – density of gas
σ – surface tension
η_C – kinematic viscosity of the liquid
θ – contact angle

1 Introduction

Designers of many devices, especially aerators and pressure aerators, need to know the mechanisms of gas bubble formation. In pressure aerators, gas is pumped under pressure into the liquid by means of diffusers containing a system of nozzles for generation of fine gas bubbles. The forming bubbles have different concentrations and shapes, which are relative to the nozzle diameter. In the case of a single hole, big bubbles are formed, and they cause pulsation. In the case of perforated grates, much smaller bubbles are generated, and they coalesce at some distance from the nozzle. The smallest bubbles form in the case of the porous plate, but it requires high gas overpressure, therefore, this type of situation is rare in industry. Under low rate of gas discharge from the nozzle, bubbles are ball-shaped and they develop at the nozzle edge [1]. In practice, such phenomena occur only in the case of gravitational gas discharge. As the gas flow rate increases, the diameter of the forming gas bubble is dependent not only on the hole diameter, but the volumetric gas flow intensity as well. For larger gas flow rates, phenomena caused by dynamic forces are becoming dominant, and the bubbles start to form at a long distance from the nozzle. In such a case, the forces connected with surface tension start to play a less important role.

The paper describes tests of the forming gas bubbles at the nozzle with a 2 mm hole located at the bottom of the round column, whose diameter is 80 mm. An optical tomograph with five projections was used for measurements of volumes of the forming bubbles [2,3]. The test results were compared with theoretical relationships known from literature [4].

2 The models of bubble formation

The problem of gas bubble formation was limited to the nozzle with a single circular hole, and the forming bubbles flow upward. It was also assumed that the bubbles are formed in the liquid in a stationary state. The literature in the field contains a variety of techniques used for modelling bubble formation process under such assumptions.

One paper [5] contains a classification of the models of bubble formation in which a distinction is made between spherical and nonspherical ones. Spherical models include such solutions in which the forming bubbles take the form of a ball. In addition, 3 types of models are distinguished, i.e., one-, two- and three-stage. This is associated with the adopted assumptions, involving the calculation of the final volume of the forming bubbles based on a single, two or three stages in which its shape is established. One stage models include static models [1] and refer to very small flows in which dynamic forces are disregarded. This group also includes models which account for dynamic forces but are based on an assumption that a bubble takes the form of a sphere which continuously increase its volume. The most popular ones include models by Davidson and Schuler [6,7], Hayes [8] and Swope [9]. Two-stage models are the ones based on the foundation that the separation of the bubble occurs in two phases. The first one includes the formation of a bubble and is followed by another in which the bubble separates. The most familiar models are ones due to Ramakrishnan-Kumar-Kuloor [10], Tsuge and Hibino [11], Miyahara [12], Gaddis and Vogelpohl [13] and Wraith [14]. Three-stage models are based on the assumption that after the separation of a bubble from the nozzle it remains in a stationary state for some time, i.e., the increase of the volume of residual gas does not occur in the nozzle after the separation of the bubble. The familiar models include the ones developed by Kupfererg and Jameson [15] and Tsuge and Hibino [16]. An assumption is made in nonspherical models that the shape of the forming bubble is dependent on the distribution of pressures along its surface. The most common models can be referred to Tan and Harris [17,18], Hooper [19], Marmur and Rubin [20]. In paper [21] there is an additional distinction made between quasi-spherical models, examples of which include ones developed by Pinczewski [22,23], Taresaka and Tsuge [24], and Yoo [25].

This paper includes a proposition of a static model additionally supplemented by inertia forces, which can be classified as a spherical one-stage model. The undertaken calculations include the void fraction of the forming bubbles and the results are compared with the results of measurements from

experiment. Additionally, a comparison is made with the selected models known from literature.

The static model completed with the dynamic forces static models, i.e., the ones which do not account for the operating inertia forces can have application only to very small gas flow rates [26,27]. For the case of larger gas streams it is necessary to consider also the dynamic phenomena in the process of gas bubble formation as the dynamic forces start to play a significant role in it. In the developed model an assumption is made that the bubbles are formed on the edge of the nozzle and they are not affected by the bubbles which were formed before, and the surrounding liquid is in the stationary state. In addition, it is assumed that the volume of the gas which originates in the nozzle results in the increase of the volume of the bubble and forces associated with the compressibility of gas are disregarded. The distribution of the forces acting on the bubble is presented in Fig. 1. These forces can be classified either as static or dynamic. Static forces include buoyancy force, surface tension force and hydraulic head force. Dynamic forces are associated with the velocity at which the center of the bubble mass moves. They include the inertia force of the mass and drag forces. The proposed model of gas bubble formation was based on the balance of forces acting on a bubble. On its basis it is possible to derive the diameter of the forming bubble under the assumption that it is round and the instant when the bubble separates coincides with the balance forces equal to zero. The equation of the balance of forces takes the following form:

$$F_B - F_\sigma - F_I - F_D - F_p = 0 \; . \tag{1}$$

Buoyancy force F_B is expressed as the mass of the liquid with the volume of the gas bubble minus its weight. It is derived from the following relation:

$$F_B = \frac{\pi d^3}{6}(\rho_l - \rho_g) \; , \tag{2}$$

where: ρ_l – density of liquid, ρ_g – density of gas, g – gravitational acceleration, d – bubble diameter.

Surface tension force F_σ acts in the tangential direction of the bubble surface at the contact point between the bubble and the edge of the hole (Fig. 1). Buoyancy force is counteracted only by the component of the vector of surface tension force and therefore, the formula for the surface tension force it is accounted for by means of the contact angle

$$F_\sigma = \sigma \pi d_o \sin\theta \; , \tag{3}$$

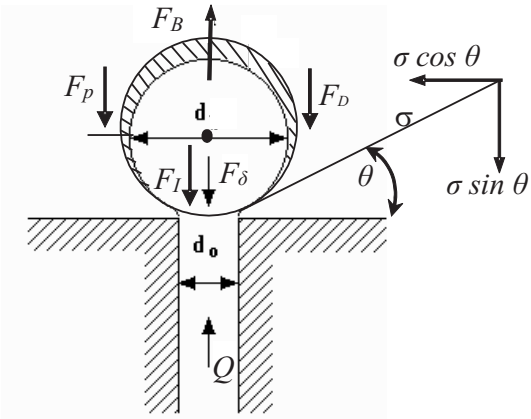

Figure 1: Static model with the dynamic forces of gas bubble formation.

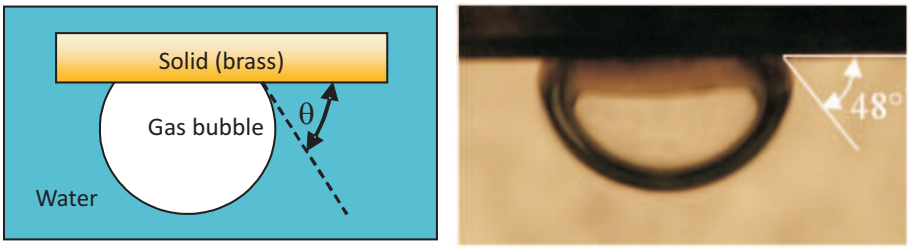

a) b)

Figure 2: Measurement of contact force: a) idea of the measurement b) bubble image.

where: σ – surface tension, d_o – orifice diameter, θ – contact angle.

The contact angle is defined in terms of the components of the surface tension force. Its value is dependent on the surface tension forces acting between the liquid and gas, gas and material from which the nozzle is made and the material used for nozzle construction (Fig. 2a). In the experiment, a brass nozzle was applied and the contact angle was determined on the way of an experiment, on the basis of photos taken from bubbles which were attached to a brass plate immersed in water (Fig. 2b). A series of such experiments was undertaken and the mean value of the contact angle was determined to be equal to 48°.

Inertia force F_I – force which is defined as the volume of the bubble with the density of the liquid which is transferred along it. The literature of the subject often defines the apparent mass to be equal to 11/16 of the

volume of the bubble [28]. This relation is accounted for in the equation to which inertia of the gas is added

$$F_I = \left(\frac{11}{16}\rho_l + \rho_g\right)\frac{\pi d^3}{12}\frac{dv}{dt} = \left(\frac{11}{16}\rho_l + \rho_g\right)\frac{2Q^2}{3\pi d^2}\ , \tag{4}$$

where: v – velocity of bubble mass center, t – time, Q – gas flow.

Drag force F_D is associated with the velocity with which the mass center of the bubble is displaced. It is defined as follows:

$$F_D = C_D\rho_l\frac{Q^2}{8\pi d^2}\ , \tag{5}$$

where C_D is the drag coefficient. In the literature it is defined in different manners [28,29,30]. The relations adopted for the purposes of this paper are taken from [12], where the drag force for bubbles with a ball shape of is defined as

$$C_D = \frac{24}{\mathrm{Re}}(1 + 0.15\,\mathrm{Re}^{0.687})\ ,\ \text{for Re} < 1000 \tag{6}$$

and

$$C_D = 0.44\ ,\ \text{for Re} > 1000\ ,$$

where Re denotes the Reynolds number, which is defined in the following way:

$$\mathrm{Re} = \frac{vd\rho_l}{\eta_l}\ , \tag{7}$$

η_C is the kinematic viscosity of the liquid.

Liquid pressure force F_p is a force resulting from the pressure of liquid above a bubble. Due to the adopted assumption of a spherical shape of the bubble, the greatest cross-section area is found in the middle of its height, which corresponds to the half of its diameter. The formula expressing the pressure force for such assumptions takes the form

$$F_p = \frac{\pi}{8}(d^3 - d_o^2 d)\rho_l g\ . \tag{8}$$

2.1 The Davidson-Schuler model

The Davidson-Schuler is based on the balance of forces acting on the bubble while the bubble volume increases continuously. It is assumed that the bubble takes the shape of a sphere, and separation of the bubble from the

nozzle takes place at the instant when the bubble centre is displaced at the distance equal to the sum of the hole radius and the bubble radius. Uplift pressure force and inertia of the liquid film moving along the bubble are the most important forces. Under such assumptions, the equation proposed by the authors takes the following form [6,31]:

$$V_b(\rho_l - \rho_g)g = \frac{d}{dt}\left\{\left(\frac{11}{16}\rho_l + \rho_g\right)V_b\frac{dx}{dt}\right\}\ , \tag{9}$$

where x is the distance between the bubble centre and the nozzle.

For a given gas flow rate at the moment of the gas bubble separation from the hole its volume is determined by the equation:

$$V_b = 1.378Q^{6/5}g^{-3/5}\ . \tag{10}$$

2.2 The Ramakrishnan-Kumar-Kuloor model

The model assumes two stages of the bubble formation. The first stage of growth assumes that the bubble forms at the hole edge and gradually increases its volume. The bubble shape is close to a sphere. If the forces displacing the bubble upward are greater than the forces acting on the bubble downward, the second stage (i.e., stage of separation of the bubble from the hole) starts. At this stage the so-called gas neck forms; it sustains the contact of the bubble with the hole. The moment when the bubble separates occurs when the length of gas neck becomes equal to length of the bubble radius, r_I, in the last phase of its growth [32,33,34]. The balance equation of forces acting on the bubble is used for determination of the final volume of the first stage

$$V_{bI}^{5/3} = \frac{11q_g^2}{192\pi\left(\frac{3}{4\pi}\right)^{2/3}g} + \frac{3\eta_l q_g V_{pI}^{1/3}}{2\left(\frac{3}{4\pi}\right)^{2/3}\rho_l g} + \frac{\pi d_o\sigma_l\cos\theta V_{bI}^{2/3}}{g\rho_l}\ , \tag{11}$$

where θ is the contact angle.

The final volume of the bubble, V_{bII}, after separation from the nozzle is calculated from the following equation [33]:

$$\sqrt[3]{\frac{3}{4}\frac{V_{bl}}{\pi}} = \frac{B}{2q_g(A+1)}\left(V_{bII}^2 - V_{bI}^2\right) - \\ -\frac{C}{q_g A}\left(V_{bII} - V_{bI}\right) - \frac{3D}{2q_g\left(A-\frac{1}{3}\right)}\left(V_{bII}^{2/3} - V_{bI}^{2/3}\right)\ , \tag{12}$$

where r_I is the final radius of the bubble in the first phase of formation,

$$r_I = \sqrt[3]{\frac{3}{4}\frac{V_{bl}}{\pi}}\ , \quad A = 1 + 1.25\frac{6\pi r_I \eta_l}{q_g\left(\rho_g = \frac{11}{16}\rho_l\right)} \approx 1 + \frac{120\pi r_I \eta_l}{11\rho_l q_g}\ ,$$

$$B = \frac{(\rho_g + \rho_l)g}{q_g\left(\rho_g + \frac{11}{16}\rho_l\right)} \approx \frac{16g}{11q_g}\ , \ C = \frac{\pi d_o \sigma_l \cos\theta}{q_g\left(\rho_g + \frac{11}{16}\rho_l\right)} \approx \frac{16\pi d_o \sigma_l \cos\theta}{11\rho_l g_g} \tag{13}$$

$$D = \frac{3\eta_l}{2\left(\frac{3}{4\pi}\right)^{1/3}\left(p_g + \frac{11}{16}\rho_l\right)} \approx \frac{24\eta_l}{11\rho_l\left(\frac{3}{4\pi}\right)^{1/3}}\ . \tag{14}$$

2.3 The Swope model

This model is a very simple one. It is based on the dimensionless equation for determination of the bubble diameter [9]:

$$\mathrm{Fr}\, d_E^5 + \left(1 - \frac{1}{\mathrm{We}}\right) d_E^2 + \left(\frac{1}{\mathrm{We}} - \frac{1}{\mathrm{Re}}\right) d_E - \frac{1}{12} = 0\ , \tag{15}$$

where $d_E = \frac{d_p}{d_o}$ is the dimensionless diameter of the bubble, and

$$\mathrm{Fr} = \frac{g\pi^2 d_0^5(\rho_l - \rho_g)}{25\rho_l Q^2}\ , \quad \text{Froude number;}\ , \tag{16}$$

$$\mathrm{We} = \frac{4\rho_g Q^2}{\pi^2 d_0^3 \sigma_l}\ , \quad \text{Weber number,} \tag{17}$$

$$\mathrm{Re} = \frac{3\rho_g Q(\mu_l + \mu_g)}{d_o \mu_l \pi(2\mu_l + 3\mu_g)}\ , \quad \text{Reynolds number.} \tag{18}$$

3 Measuring system

The measuring system includes an optical tomograph with a scattered light beam [2]. The beam is emitted from a single point light source, and next detection is made within the radius of the beam scattering (Fig. 3a).
The system used in the measurements included a 76 mm diameter pipeline. Five light sources were located around the pipeline. A light source was a 55 W light bulb. The scanning planes were arranged at different distances along the pipeline axis, so it was possible to determine velocities of the moving objects. Sixty four phototransistors were used as detectors of the light beam for each of the five projections.

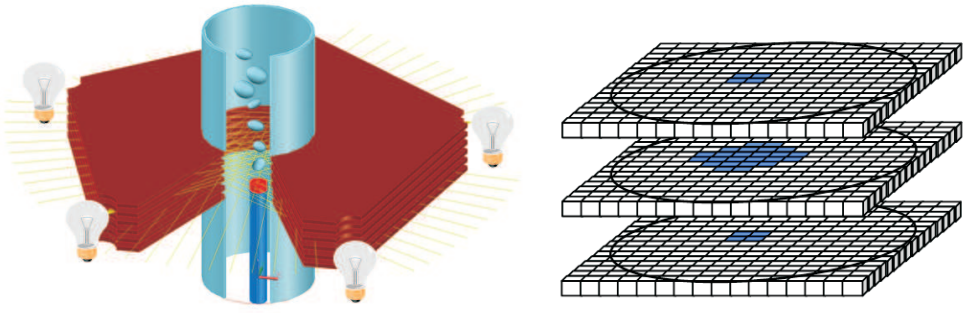

a) b)

Figure 3: Optical tomograph: a) structure of the measuring system, b) idea of the shape reconstruction.

The measuring space of the tomograph was filled with water where a nozzle with a 2 mm diameter hole was placed. Air was delivered from a gas cylinder, and the gas stream was measured by means of an electronic flow sensor. The image reconstructed by the tomograph includes a regular net, particular pixels of which define the area which is occupied by gas. Each successive frame of the image is registered with a constant time step (Fig. 3b). Thus, it is possible to reconstruct bubble shape and calculate its volume.

4 Results of measurements of the forming bubble shape

For low gas flow rates, the bubbles are spherical and they form at the nozzle edge. In practice, such phenomena take place only for the case of the gravitational gas flow. As the gas flow rate increases, the diameter of the forming bubble does not only depend on the hole diameter but the value of the volumetric gas flow rate as well.

In the case of very small flow rates, the bubbles separate as groups of a few or several bubbles, and next there is a break in their emission. As the gas flow rate increases, the breaks become shorter and the number of bubbles in one group increases. Bubbles take a characteristic spherical shape with a cylindrical foot at the bottom (Fig. 4). As the gas stream increases, this part becomes longer causing increase of the volume of the forming bubble.

An increase of the gas stream from the nozzle results in an increase of the influence of dynamical forces acting on forming bubbles. Consequently,

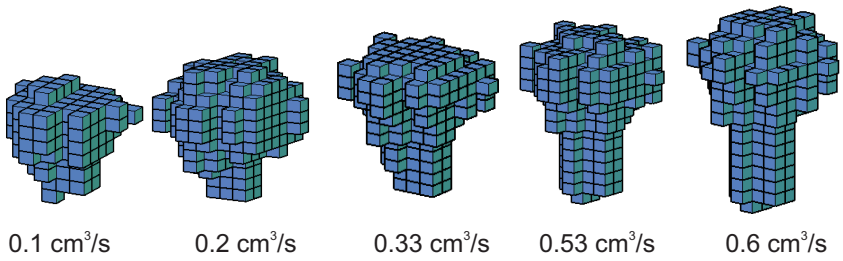

Figure 4: Results of measurements of the bubble shapes for the unrestricted flow ($\mathrm{Re} < 1.4 \times 10^{-4}$, $\mathrm{Fr} > 400$).

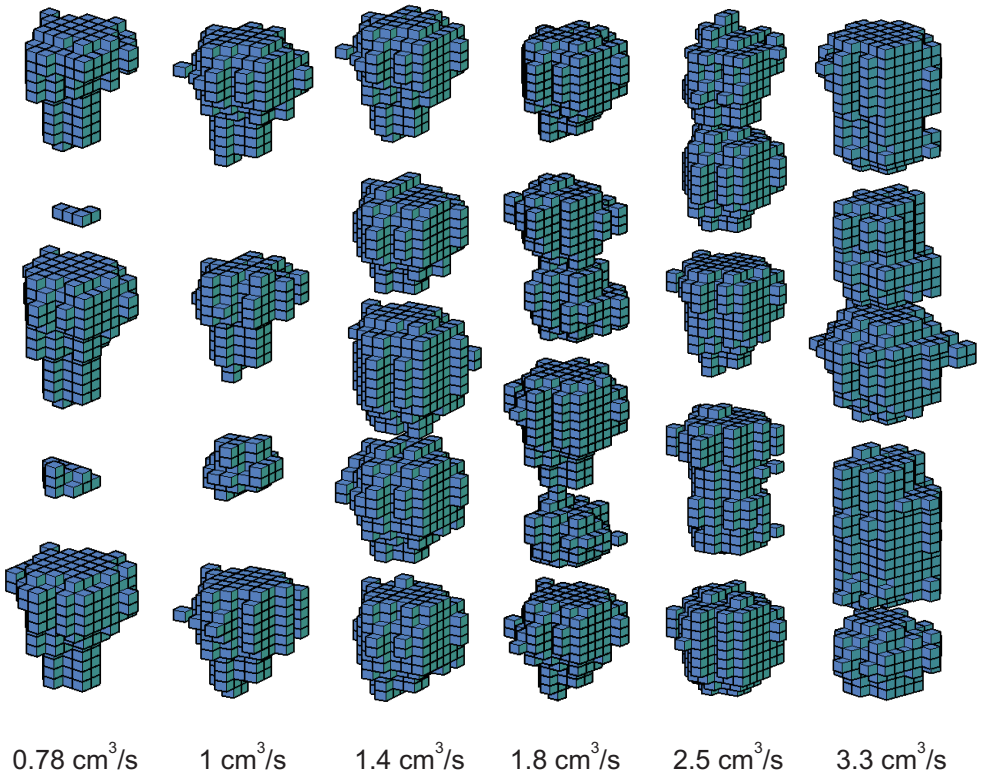

Figure 5: Results of measurements of the bubble shapes for the transient flow ($1.4 \times 10^4 < \mathrm{Re} < 9 \times 10^{-4}$, $400 > \mathrm{Fr} > 10$).

an increase of the diameter of the spherical part occurs accompanied by a decrease of the cylindrical part (Fig. 5). It is caused by the fact that the gas flowing with a high velocity has a greater resistance to motion.

The liquid swirls caused by such gas flow affect the formation of successive bubbles and lead to differences in volumes and shapes of the separating bubbles. We can observe the formation of the spherically-shaped bubbles with no cylindrical parts. It is a beginning of the transient state leading to formation of the chain of bubbles.

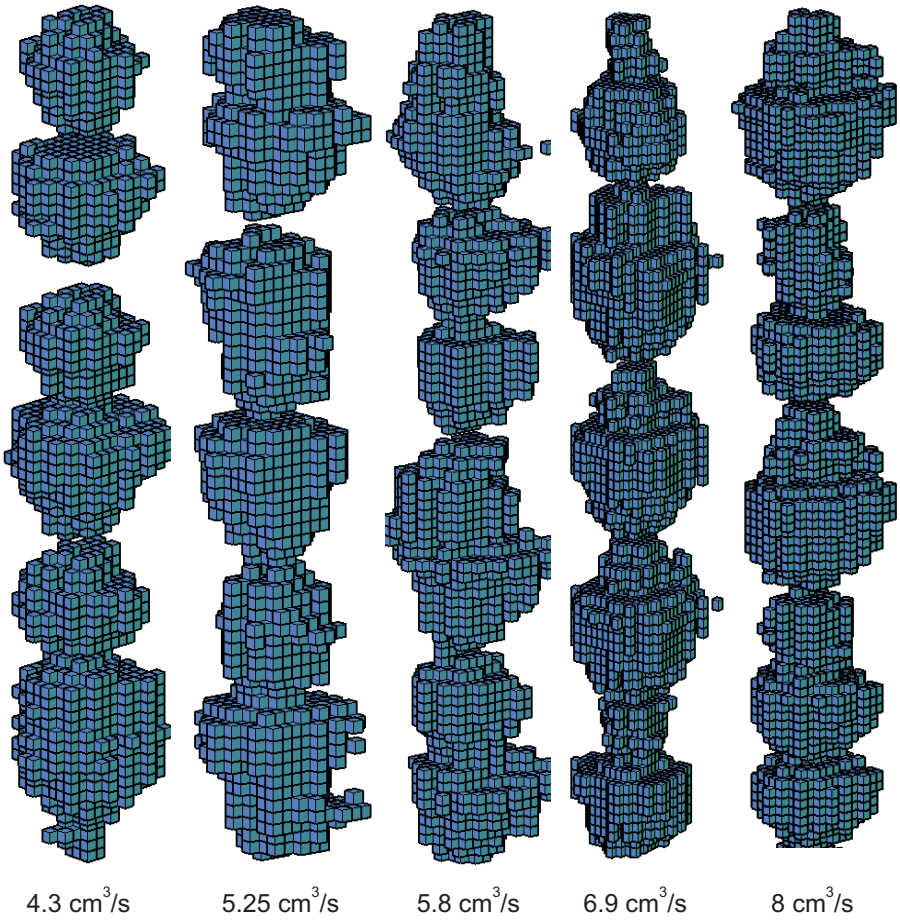

Figure 6: Results of measurements of the bubble shape for the chain flow ($\mathrm{Re} > 9 \times 10^{-4}$, $\mathrm{Fr} < 10$).

During the transient flow, the increase of the gas stream does not affect a significant change of the diameter of the spherically-shaped parts of the forming bubbles. However, it is reflected in the intensity of bubble formation. Bubbles forming over a short time, one by one, result in liquid

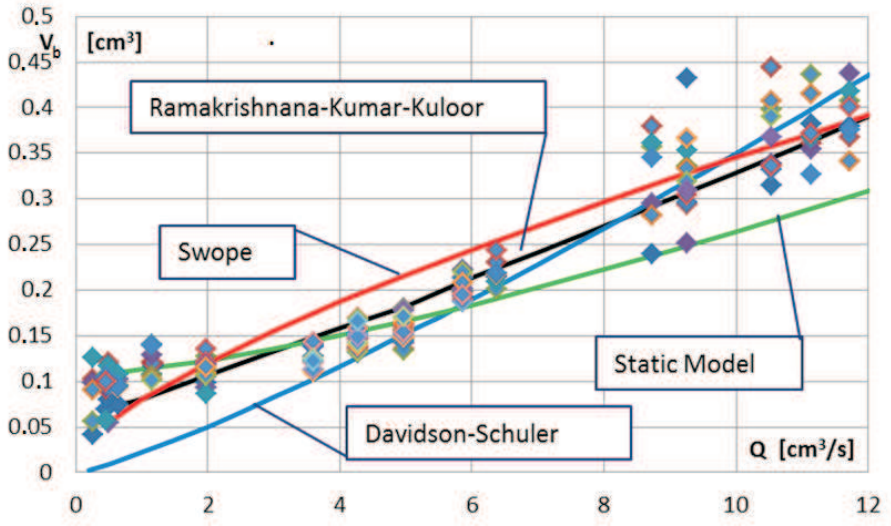

Figure 7: Comparison of the measuring results obtained for volumes of the forming bubbles with theoretical models.

circulation in the surroundings of the forming bubbles. As a consequence, additional forces originate which deform the forming bubbles. The irregularity in bubble formation and the gas flow increase become more intense, and the cylindrical part decays.

As the gas stream increases, turbulence of bubble formation increases as well. It is more difficult to define the point where the bubbles separate. At the nozzle tip there is a continuous gas flux which takes different shapes. We can observe characteristic chains which separate from the nozzle. Next, while they are in motion, they separate into successive bubbles. The characteristic formation of the chains is presented in Fig. 6. As the gas stream increases, intensity of the bubble chain separation increases, too.

The experimental results obtained by applied method are shown in Fig. 7. The experimental data were compared with the theoretical models. Some divergences of the measuring results for greater gas flow rates can be explained by non-stationary course of phenomena occurring during bubble formation.

5 Comparison between theoretical and experimental bubble formation

Theoretical models were compared with experimental results obtained by this method (Fig. 7). The bubble volumes for different gas streams were measured by means of an optical tomograph, and three-dimensional images were applied for the calculations of the volumes of particular bubbles. In the figure above, the solid lines denote the calculation results for the static model and models proposed by Davidson-Schuler, Ramakrishnan-Kumar-Kuloor and Swope. The theoretical results are different depending on a particular model. The static model can be applied only in the case of free formation of bubbles. The experimental points overlap with the results known from literature. It proves the correctness of the developed models and convergence with the theoretical data. The Davidson-Schuler reflects well the experimental data for greater values of the gas flow rates. For the case of the very slow rate of the gas it tends to indicate a lower volume of the bubbles. For the case of small and large gas streams a good approximation can be achieved by the application of the Swope model. However, this model indicates a considerably different curve of the bubble volume in relation to the data gained from experiments, in the middle part of the chart in Fig. 7. A good conformity of the results with experimental data was achieved for the Ramakrishnan-Kumar-Kuloor model. However, this model is based on a two-stage process of calculating the volume fraction of the bubbles. On this basis a conclusion can be made that one is justified to search for one-stage models, as they are able to approximate the values of the bubble volume for small flow rates of gas. The proposed static model accounting for dynamic forces confirms that the values from calculation overlap with the experimental results for small gas rates in the range up to 5 cm^3/s. This function offers a satisfactory conformity with experimental data. By comparing the results of the research one can conclude that among the discussed theoretical models in the range up to 5 cm^3/s the static model offers the biggest conformity of the results. For the range of the greater gas rates it requires some modifications to be introduced. The models assume bubble formation in a motionless water, and in practice, for great flow rates of gas, water does not remains at rest, but successive bubbles cause its circulation.

6 Conclusions

The method of optical tomography was used for the measurement of both the shape and velocity of the bubbles formed at the outlet of circular nozzle in a plate. In this way, it is possible to find the relation between the gas stream and the volume of bubbles. The experimental results have allowed verification of the known theoretical models.Optical tomography can be applied for research into gas bubbles forming at the slot or other devices for bubble distribution.

Received 15 October 2012

References

[1] Orzechowski Z.: *One-dimensional two-phase flows established adiabatically*. PWN Warsaw 1990 (in Polish).

[2] Rząsa M.R., Grudzień K., Przywarski R., Romanowski A., Wajman R.: *The Discrete Optical Tomograph Including Five Projections*. In: Proc. 5th World Congress on Industrial Process Tomography, Bergen 2007.

[3] Rząsa M.R., Pląskowski A.: *Application of optical tomography for measurements of aeration parameters in large water tanks*. Meas. Sci. Technol. **14**(2003), 2, 199–204.

[4] Dziubiński M., Prywer J.: *Mechanics of two-phase fluids*. WNT, Warszawa 2010 (in Polish).

[5] Xiao Z.: *Bubble Formation and Bubble-wall Interaction at a Submerged Orifice*. Nation University of Singapore, 2004.

[6] Davidson J. F., Schuler B.O.: *Bubble formation at an orifice in a viscous liquid*. T. Inst. Chem. Engender. **38**(1960), 144–154.

[7] Davidson J. F., Schuler B.O.: *Bubble formation at an orifice in an inviscid liquid*. T. Inst. Chem. Engender. **38**(1960), 335–342.

[8] Hayes W.B., Hardy B.W., Holland C.D.: *Formation of gas bubbles at submerged orifices*. A.I.Ch.E. J. **5**(1959), 3, 319–324.

[9] Swope R.D.: *Single bubble formation at orifices submergedin viscous liquids*. J. Chem.Eng.**49**(1971), 169–174.

[10] Ramakrishnan S., Kumar R., Kuloor N.R.: *Studies in bubble formation-I. Bubble formation under constant flow conditions*. Chem. Eng. Sci. **24**(1969), 731–747.

[11] Tsuge H., Hibino S.: *Bubble formation from a submerged single orifice accompanied by pressure fluctuations in gas chamber*. J. Chem. Eng. Japan **11**(1979), 3, 173–178.

[12] Miyahara T., Matsuba Y. and Takahashi T.: *Bubble formation from an orifice at high gas flow rates*. Int. Chem. Eng. **23**(1983), 3, 524–531.

[13] Gaddis E. S., Vogelpohl A.: *Bubble formation in quiescent liquids under constant flow conditions*. Chem. Eng. Sci. **41**(1986), 1, 97–105.

[14] Wraith A.E.: *Two-stage bubble growth at a submerged plate orifice*. Chem. Eng. Sci. **26**(1971), 1659–1671.

[15] Kupferberg A., Jameson G.J.: *Bubble formation at submerged orifice above a gas chamber of finite volume*. Trans. Inst. of Chem. Eng. **47**(1969), 241–250.

[16] Tsuge H., Hibino S.: *Bubble formation from an orifice submerged in liquids*. Chem. Eng. Commun. **22**(1983), 63–79.

[17] Tan R.B.H., Chen W.B., Tan K.H.: *Non-spherical model for bubble formation with liquid cross-flow*. Chem. Eng. Sci. **55**(2000), 6259–6267.

[18] Tan R.B.H., Harris I.J.: *A model for non-spherical bubble formation at a single orifice*. Chem. Eng. Sci. **41**(1986), 12, 3175–3128.

[19] Hooper A.P.A.: *A study of bubble formation at a submerged orifice using the boundary element method*. Chem. Eng. Sci. **41**(1986), 1879-1890.

[20] Marmur A., Rubin E.: *A theoretical model for bubble formation at an orifice submerged in an inviscid liquid*. Chem. Eng. Sci. **31**(1976), 453–463.

[21] Zhang Y.: *Modeling the Effect of Liquid Viscosity and Surface Tension on Bubble Formation*. Nation University of Singapore, 2004.

[22] Pinczewski W.V.: *The formation and growth of bubbles at a submerged orifice*. Chem. Eng. Sci. **36**(1981), 405–411.

[23] Zughbi H.D., Pinczewski W.V., Fell C.J.: *Bubble growth by the marker and cell technigue*. In: Proc.8th Australian Fluid Mechanics Conf. 1983, 8B.9–8B.12.

[24] Teresaka K., Tsuge H.: *Bubble formation at a single orifice in highly viscous liquids*. J. Chem. Eng. Jpn **23**(1990), 160–165.

[25] Yoo D., Teresaka K., Tsuge H.: *Behavior of bubble formation at elevated pressure*. J. Chem. Eng. Jpn **31**(1998), 1, 76–82.

[26] Rząsa M.R.: *The dynamic flow meter for uses of measurement a very small gas flow*. In: Proc. IV Sympozjum nt. Pomiarów dynamicznych, Gliwice, 7-8 Nov. 2002.

[27] Rząsa M.R., Sawicki J.: *A flowmeter for measurements of very small gas flows*. Sensor. Transducer. Mag. **40**(2004), 2, 128–136.

[28] Zhang L., Shoji M.: *Aperiodic bubble formation from a submerged*. Chem. Eng. Sci. **56**(2001), 5371–5381.

[29] Dijkhuizen W., Sint Annaland M,. Kuipers. J.A.M.: *Direct numerical simulation of the drag force in bubble swarms*. 6th Int. Conf. Multiphase Flow, Leipzig, July 9-13, 2007.

[30] Loubiere K., Hebrard G.: *Bubble formation from a flexible hole submerged in an inviscid liquid*. Chem. Eng. Sci. **58**(2003), 135–148.

[31] Davidson J.F., Mech A.M.I., Schuler B.O.G.: *Bubble formation at an orifice in a viscous liquid*. Chem. Eng. Res. Des. **75**(1997), Sup. 1, S105–S115.

[32] Khurana A.K., Kumar R.: *Studies in Bubble Formation-III*. Chem. Eng. Sci. **24**(1969), 1711–1723.

[33] Kumar R., Kuloor N.R.: *The formation of bubbles and drops.* Advances in Chem. Eng. **8**(1970), 255–368.

[34] Satyanarayan A., Kumar R., Kuloor N.R.: Studies in Bubble Formation - II. Bubble Formation under Constant Pressure conditions. Chem. Eng. Sc. **24**(1969), 749–761.7